Semiclassical Limit of a Measurement-Induced Transition in Many-Body Chaos in Integrable and Nonintegrable Oscillator Chains

Sibaram Ruidas⊚* and Sumilan Banerjee†

Centre for Condensed Matter Theory, Department of Physics, Indian Institute of Science, Bangalore 560012, India

We discuss the dynamics of integrable and nonintegrable chains of coupled oscillators under continuous weak position measurements in the semiclassical limit. We show that, in this limit, the dynamics is described by a standard stochastic Langevin equation, and a measurement-induced transition appears as a noise- and dissipation-induced chaotic-to-nonchaotic transition akin to stochastic synchronization. In the nonintegrable chain of anharmonically coupled oscillators, we show that the temporal growth and the ballistic light-cone spread of a classical out-of-time correlator characterized by the Lyapunov exponent and the butterfly velocity are halted above a noise or below an interaction strength. The Lyapunov exponent and the butterfly velocity both act like order parameter, vanishing in the nonchaotic phase. In addition, the butterfly velocity exhibits a critical finite-size scaling. For the integrable model, we consider the classical Toda chain and show that the Lyapunov exponent changes nonmonotonically with the noise strength, vanishing at the zero noise limit and above a critical noise, with a maximum at an intermediate noise strength. The butterfly velocity in the Toda chain shows a singular behavior approaching the integrable limit of zero noise strength.

Chaotic-to-nonchaotic transitions play a prominent role in our understanding of the dynamical phase diagram of both quantum and classical systems, appearing in many different contexts such as nonlinear dynamics, thermalization, and quantum information theory. In quantum many-body systems, a certain kind of chaotic-nonchaotic transitions, dubbed "measurement-induced phase transitions" (MIPT) [1–12], have led to a new paradigm for dynamical phase transitions in recent years. These transitions are characterized by entanglement and chaotic properties of the many-body states and time evolution. On the other hand, a prominent example of transition in chaos in classical dynamical systems [13–25] are the so-called synchronization transitions (STs) [26]. In this case, classical trajectories starting from different initial conditions synchronize, i.e., the difference between the trajectories approaches zero with time, when subjected to sufficiently strong common drive, bias, or even random stochastic noise. Can there be some connection between the measurement-induced phase transition in quantum systems and ST in classical systems?

In this Letter, we establish a possible link between MIPT and ST by considering models of interacting particles, whose positions are measured continuously, albeit weakly. We show that, in the semiclassical limit, the dynamics of the system is described by a stochastic Langevin equation where the noise and the dissipation terms are both controlled by the small quantum parameter $\hbar$ and measurement strength. Specifically, we study a nonintegrable oscillator

chain and the classical integrable Toda chain [27–30]. In both cases, we find a surprising dynamical transition in many-body chaos in the Langevin evolution. The chaotic-to-nonchaotic transition occurs as a function of either interaction or noise (measurement) strength as two classical trajectories starting with slightly different initial conditions synchronize when subjected to identical noise. The transition is similar to the stochastic STs. The latter has been previously studied [19–25,31,32], however, only for lattices of coupled nonlinear maps, as opposed to interacting Hamiltonian systems employed in our Letter.

A few recent works have looked into classical analogs of MIPT in cellular automaton [33], kinetically constrained spin systems [34,35], and semiclassical circuit model [36]. In contrast to these works, we derive a direct connection between a quantum measurement dynamics of a Hamiltonian system with the Langevin evolution by analytically taking the semiclassical limit. For interacting quantum systems, MIPTs have been primarily studied in quantum circuits evolving under discrete-time projective and weak measurements [1–12] as well as continuous weak measurements [37,38]. The MIPTs in these models are typically characterized by scaling of entanglement entropy with subsystem size, i.e., transition from a volume-law to area-law scaling, in the longtime steady state. These MIPTs can often be mapped to phase transitions in some classical statistical mechanics models [1,2,6,8,10,12]. However, it is hard to directly take the classical limit of the dynamics in these quantum circuit models. Effects of measurements and

MIPTs have also been studied for noninteracting fermions [7,39,40], interacting bosons [41–43], and Luttinger liquid ground state [44].

We characterize the chaos transition in the Langevin dynamics of the oscillator chains by a classical out-of-time-order correlator (cOTOC) [45–51]. The latter is defined by comparing two trajectories that differ by a small amount initially and are subjected to identical noise. In the chaotic phase, we extract a Lyapunov exponent λ_L and a butterfly velocity v_B, respectively, from the cOTOC. We show the following. (i) $\lambda_L, v_B \to 0$ at a critical noise strength or below an interaction strength for both integrable and nonintegrable chains. (ii) v_B exhibits a critical scaling with system size, whereas λ_L shows almost no system-size dependence. The critical exponents extracted from the finite-size scaling of v_B differs from those in the universality classes typically found in stochastic STs in coupled-map lattices (CMLs) [19,20,23,25,31,32]. (iii) For the stochastic dynamics of the integrable Toda chain, λ_L changes nonmonotonically with the noise strength, vanishing for zero noise, as well as at a critical noise; v_B, on the other hand, shows a singular behavior approaching the integrable limit of zero noise strength.

Quantum measurement model and the semiclassical limit.—We generalize the well-known model of continuous weak position measurement of a single particle by Caves and Milburn [52] to the interacting oscillator chains. The oscillator chain (system) with $i = 1, \ldots, L$ oscillators and the measurement apparatus (meters) [see Fig. 1(a)] are described by the following time-dependent Hamiltonian:

$$\mathcal{H}(t) = \mathcal{H}_s + \sum_{i,n}\delta(t - t_n)\hat{x}_i\hat{p}_{in}. \tag{1}$$

The Hamiltonian of the system is $\mathcal{H}_s = \sum_i(\hat{p}_i^2/2m) + V(\{\hat{x}_i\})$, where $\hat{x}_i$, $\hat{p}_i$ are the operators for displacement of the ith oscillator from the equilibrium position and its momentum. We apply periodic boundary conditions. The potential is $V(\{x_i\}) = \sum_i v(r_i)$, with $r_i = x_{i+1} - x_i$. We take (i) $v(r) = [(\kappa/2)r^2 + (u/4)r^4]$ for the nonintegrable chain with κ spring constant and u the strength of the anharmonicity, and (ii) $v(r) = [(a/b)\exp(-br) + ar - (a/b)]$ for the integrable Toda chain [27–30,53] with parameters a and b. The displacement x_i of the ith oscillator is weakly measured by the inth meter at time $t = t_n = n\tau$ at regular intervals of τ. $\hat{p}_{in}$ is the momentum operator of the inth meter, which is in a Gaussian state $\psi(\xi_{in}) = (\pi\sigma)^{-1/4}\exp(-\xi_{in}^2/2\sigma)$ at t_n^-. At t_n, the position ξ_{in} of the meter is projectively measured and its state collapses to a position state $|\xi_{in}\rangle$. The effect of this measurement on the system is described by an operator $\Psi_i(\xi_{in}) = (\pi\sigma)^{-1/4}\exp[-(\xi_{in} - \hat{x}_i)^2/2\sigma]$ acting on the system, as described in detail in the Supplemental Material (SM), Sec. S1 [54]. In the continuous measurement limit $\tau \to 0$, $\sigma \to \infty$ such that $\Delta = \sigma\tau$ is kept fixed [52].

The mean momentum and position of the particle jump by an amount $\propto \xi_{in}$ after each measurement [52], and they can wander far away from the initial values at long times. Thus, to incorporate a feedback mechanism present in any realistic measurement setup [52] a displacement operator, $D_i(\xi_{in}) = \exp[(i/\hbar)\gamma\tau\xi_{in}\hat{p}_i]$, is applied on the system after the inth measurement, where $\gamma = c_\gamma\sqrt{2\hbar/m\Delta}$, with dimensionless coefficient c_γ. We do not need to apply a displacement operator for the position due to the periodic boundary condition. The feedback mechanism on the momentum leads to dissipation [52], as discussed below.

The density matrix of the system at t_n^+ is given by $\rho(\{\xi\}_n, t_n^+) = \mathcal{M}(\xi_n)\rho(\{\xi\}_{n-1}, t_{n-1}^+)\mathcal{M}^\dagger(\xi_n)$, which depends on the outcomes of all the measurements $\{\xi\}_n$ till t_n^+. Here $\mathcal{M}(\xi_n) = \prod_i[D_i(\xi_{in})\Psi_i(\xi_{in})]\exp(-i\mathcal{H}_s\tau/\hbar)$. For the evolution of an initial pure state, the above time evolution can be written as a quantum state diffusion [55,56]. Here we write the longtime evolution as a Schwinger-Keldysh (SK) path integral [57] for $\tau \to 0$, i.e., $\text{Tr}[\rho(\{\xi(t)\})] = \int \mathcal{D}x \exp(iS[\{\xi(t)\}, x(t)]/\hbar)$ with the action

$$S[\{\xi\}, x] = \int_{-\infty}^{\infty} dt \sum_{s=\pm} s\left[\left\{\sum_i \frac{m}{2}(\dot{x}_i^s)^2 + m\gamma\dot{x}_i^s\xi_i \right. \right.$$
$$\left. \left. + (is\hbar/2\Delta)(x_i^s - \xi_i)^2\right\} - V(\{x_i^s\})\right], \tag{2}$$

where $s = \pm$ denotes two branches of the SK contour [57], $\dot{x}_i = (dx_i^s/dt)$. To take the semiclassical limit of small $\hbar$, we rewrite the above path integral in terms of classical (x_i^c) and quantum components (x_i^q), i.e., $x_i^\pm = x_i^c \pm x_i^q$. To capture nontrivial effects of the quantum (x_i^q) fluctuations, which act as noise in the semiclassical limit, we need to scale $\Delta \sim \hbar^2$ (see SM, Sec. S1 [54]). Taking the semiclassical limit in this manner and keeping $\mathcal{O}(1/\sqrt{\hbar})$ and $\mathcal{O}(1)$ terms, we find that a Langevin equation describes the dynamics of the system,

$$\ddot{x}_i^c + \gamma\dot{x}_i^c = \frac{1}{m}\left[-\frac{\partial V(\{x_i^c\})}{\partial x_i^c} + \eta_i\right], \tag{3}$$

for the classical component x_i^c, denoted by x_i henceforth. Here the $\eta_i(t)$ is Gaussian random noise that originates from x_i^q and is controlled by the measurement strength Δ^{-1} such that $\langle\eta_i(t)\eta_j(t')\rangle = 2m\gamma T_{\text{eff}}\delta_{ij}\delta(t - t')$. $T_{\text{eff}} = (\hbar/4c_\gamma)\sqrt{\hbar/2m\Delta}$, which we denote as T in the rest of the Letter for brevity, is an effective temperature $\sim\sqrt{\hbar}$ that determines the noise strength along with γ. The latter is the effective dissipation strength $\sim 1/\sqrt{\hbar}$. In the strict classical limit $\hbar \to 0$, $T \to 0$, and $\gamma \to \infty$. As a result, the dissipative term completely dominates and the system becomes static. The nontrivial semiclassical dynamics results from keeping $\hbar$ small but nonzero. In this limit the system reaches a

longtime steady state described by classical Boltzmann-Gibbs distribution $\sim \exp\left[-\mathcal{H}_s(\{x_i, p_i\})/T\right]$ determined by the effective temperature. However, the temperature here does not arise from any external baths, but solely from the measurement and feedback process.

Classical dynamics and cOTOC.—We study the dynamics [Eq. (3)] of the nonintegrable chain as a function of both γ and u for a fixed T. The Hamiltonian is trivially integrable and nonchaotic for the harmonic chain ($u = 0$). Any nonzero u makes the model nonintegrable and chaotic. On the contrary, the classical Toda chain is integrable, albeit interacting [27–30]. We can tune the model from a harmonic limit to a hard sphere limit by changing a and b [53]. We take the parameters in the intermediate regime for the convenience of the numerical simulations.

We numerically simulate Eq. (3) and generate classical trajectories for the nonintegrable and integrable chains using the Gunsteren-Berendsen method [58]; see SM, Sec. S2 for details [54]. We characterize many-body chaos by the following cOTOC:

$$\mathcal{D}(i, t) = \langle [p_i^A(t) - p_i^B(t)]^2 \rangle. \tag{4}$$
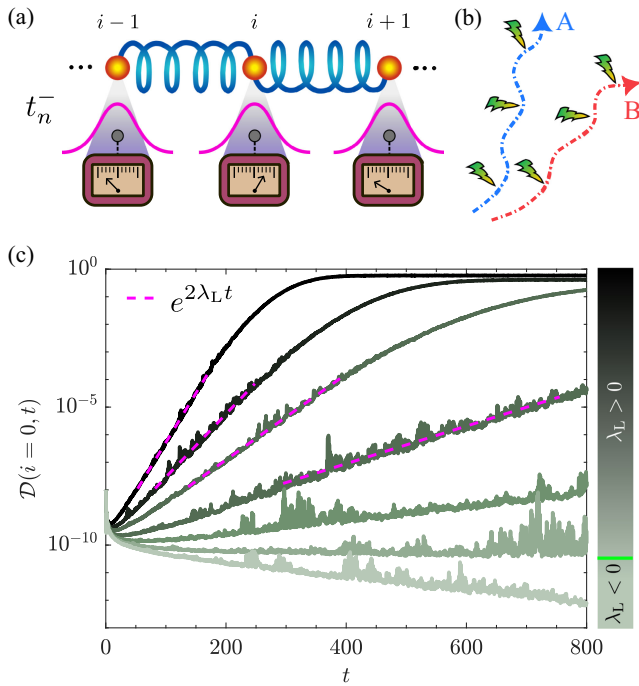

(a)
$i-1$ i $i+1$
t_n^-

(b)
A
B

(c)

FIG. 1. Measurement model and cOTOC. (a) Schematic of the measurement model, where the positions of the coupled oscillators ($i = 1, ..., L$) on a chain are weakly measured at time t_n by meters prepared in Gaussian states just before the measurements. (b) Schematic of two initially nearby classical trajectories, A and B, subjected to identical noise realizations. (c) The classical OTOC $\mathcal{D}(i = 0, t)$ as a function of u across the chaos transition for $\gamma = 0.10$ with u values 0.80 (darkest), 0.60, 0.50, 0.40, 0.35, 0.32, and 0.30 (lightest). As shown by dashed magenta lines, the cOTOC grows exponentially ($\sim e^{2\lambda_L t}$) for $u > u_c \simeq 0.32$, whereas it decays exponentially for $u < u_c$ in the synchronized phase.

Here A and B are two trajectories of the system generated from initial thermal equilibrium configurations $\{x_i^A(0), p_i^A(0)\}$ for $T = 1$ with $p_i^B(0) = p_i^A(0) + \delta_{i,0}\varepsilon$ ($\varepsilon = 10^{-4}$); $\langle \cdots \rangle$ denotes average over thermal initial configurations (see SM, Sec. S3 for details). We use 10^5 initial configurations for all our results. We use identical noise realization for the two copies at each instant of time, i.e., $\eta_i^A(t) = \eta_i^B(t)$, as in the earlier studies of stochastic STs and CMLs [19–25,31,32].

Results.—For $\gamma = 0$, the nonintegrable chain is chaotic, i.e., the cOTOC grows exponentially for any value of u, except the harmonic limit $u = 0$ (Fig. S2 of SM [54]). However, for $\gamma \neq 0$, the system is chaotic only above a critical value u_c of the interaction, as shown in Fig. 1(c). The cOTOC decays exponentially ($\lambda_L < 0$) for $u < u_c$, instead of growing. This is the stochastic ST. Similar transition is seen as a function of noise strength γ for a fixed $u \neq 0$ (Fig. S1 of SM). The exponential growth is concomitant with a ballistic light cone in cOTOC, whereas the light cone is destroyed in the nonchaotic phase, as shown in Figs. 2(a) and 2(b).

We extract the Lyapunov exponent λ_L from $\mathcal{D}(0, t) \sim \exp(2\lambda_L t)$. The results for λ_L as a function of u for a few γ, and as a function of γ for $u = 1$, are shown in Figs. 2(c) and 2(d), for different system sizes $L = 256, 512, 800, 1024$. It is evident that λ_L approaches zero at a critical value u_c or γ_c, becoming negative for $u < u_c$ ($\gamma > \gamma_c$), and λ_L has little L
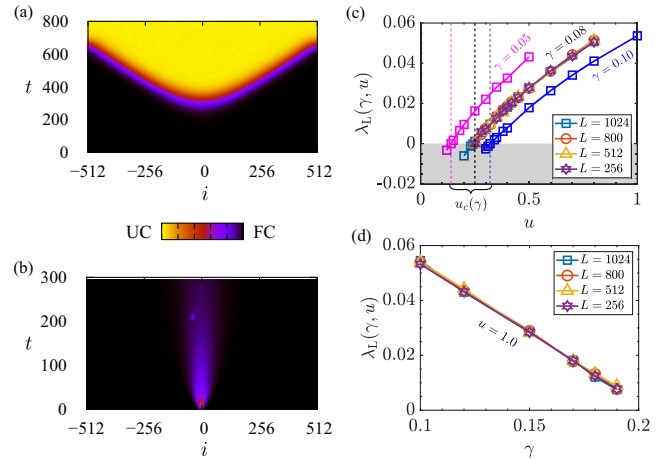

FIG. 2. Ballistic light-cone spreading and Lyapunov exponent across the chaos transition. (a) Light cone for $u = 0.80 > u_c$ and $\gamma = 0.10$. The color represents the value of the cOTOC $\mathcal{D}(i, t)$ as function of lattice site i and time t, as indicated in the color bar from small $\mathcal{D}(i, t)$ or fully correlated (FC) to large $\mathcal{D}(i, t)$ or uncorrelated (UC). (b) The light-cone spreading ceases in the nonchaotic phase for $u = 0.30 < u_c$ and $\gamma = 0.10$. (c) λ_L as a function of u for different γ's and system sizes L. λ_L approaches zero at the critical interactions $u_c = 0.14, 0.25$, and 0.32 (dashed lines) for $\gamma = 0.05, 0.08$, and 0.10, respectively, for the chaos transition. The shaded region marks $\lambda_L < 0$. (d) Similar transition is observed as a function of noise strength γ at $\gamma_c \simeq 0.20$ for $u = 1$, as shown for different L's.
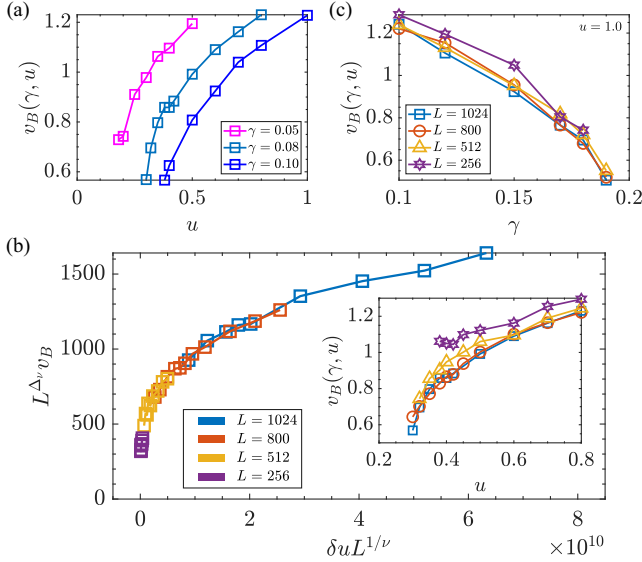
FIG. 3. Butterfly velocity and finite-size scaling in the nonintegrable chain. (a) v_B as a function of u for different noise strength γ. (b) The system size (L) dependence of $v_B(u)$ is shown for $\gamma = 0.08$ in the inset, and the finite-size scaling collapse is shown in the main panel with exponents $\Delta_v = 1.04$ and $\nu = 0.27$ for $u_c = 0.24$. (c) v_B as a function of γ for $u = 1.0$ for different L's.

FIG. 4. Transitions in many-body chaos in Toda model. (a) Lyapunov exponent λ_L and (b) butterfly velocity v_B as function of noise strength γ for different system sizes. For $\gamma \to 0$, $\lambda_L \sim \gamma^{0.26}$ as shown by the dashed line in (a). The shaded region in (a) corresponds to $\lambda_L < 0$. The chaos transition occurs around $\gamma_c \simeq 3.30$ (dashed line) for both λ_L and v_B.

dependence. Hence the semiclassical limit [Eq. (3)] of the quantum measurement dynamics described by the action in Eq. (2) indeed yields an ST as a function of the interaction and γ. Since $\gamma \sim 1/\sqrt{\Delta}$, ST is controlled by the measurement strength Δ^{-1}, which determines how precisely the oscillator positions are measured. As a result, based on its microscopic origin from a quantum measurement model [Eq. (1)], the ST in this case can be termed as an MIPT, albeit in the semiclassical limit. The transition appears to be continuous, though it is hard to extract λ_L accurately close to the transition.

The ballistic spreading of cOTOC is quantified by extracting butterfly velocity v_B, e.g., from the light cones of Fig. 2(a) (see SM, Sec. S4 for details [54]). v_B decreases approaching the transition from the chaotic phase, as shown in Figs. 3(a) and 3(c), as a function of u and γ, respectively. However, close to the transition, the light cone becomes progressively ill defined and we could not extract v_B all the way up to the transition. Unlike λ_L, v_B shows perceptible and systematic L dependence [Fig. 3(b) (inset)], especially for the transition as a function of u. Thus we perform a finite-size scaling analysis of the data for $\gamma = 0.08$, where we collapse the data for different L and $\delta u = (u - u_c) > 0$ using $v_B(u, L) = L^{-\Delta_v} \mathcal{F}((\delta u)L^{1/\nu})$. Here $\mathcal{F}(x)$ is a scaling function (SM, Sec. S5). Reasonably, good scaling collapse is obtained with $\Delta_v \simeq 1.03 \pm 0.03$ and $\nu \simeq 0.30 \pm 0.05$, for the range $u_c = 0.21$–0.25, which is close to the $u_c \simeq 0.25$ obtained from λ_L in Fig. 2(c). The scaling form implies that for $L \to \infty$, $v_B \sim (\delta u)^\beta$ with $\beta = \nu \Delta_v \simeq 0.28$, and a correlation length ξ diverges as
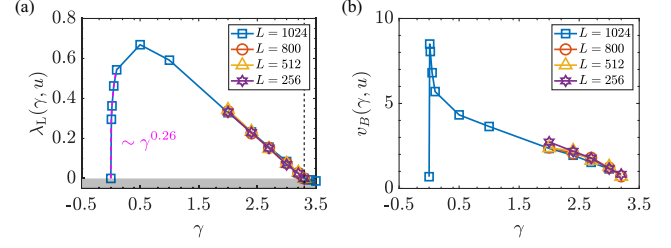
$(\delta u)^{-\nu}$ in the chaotic phase. The correlation length exponent $\nu \simeq 0.3$ is different from that for the usual universality classes of STs, such as multiplicative noise or directed percolation, found in earlier studies in CMLs [19,20,23,25,31,32], cellular automaton [33], and kinetically constrained model [34,35]. We note that exponents different from the known universality classes have been found for some cases in previous works on CMLs as well [20].

The dynamical transition in the stochastic evolution of a nonintegrable oscillator chain is not seen in the usual dynamical properties of a single trajectory. It can only be detected through many-body chaos by comparing two trajectories. To confirm this, we compute the average mean-square displacement (MSD) for the trajectories, i.e., $\langle \Delta q^2(t) \rangle = (1/N) \sum_i \langle [x_i(t) - x_i(0)]^2 \rangle$ (SM, Sec. S6 [54]). For $\gamma = 0$, in the harmonic chain ($u = 0$) with periodic boundary condition, $\langle \Delta q^2(t) \rangle \sim t$ exhibits a diffusive behavior as shown in Ref. [59]. The diffusive behavior persists for $u \neq 0$ and $\gamma = 0$. However, turning on $\gamma \neq 0$, dynamics becomes subdiffusive with $\langle \Delta q^2(t) \rangle \sim \sqrt{t}$ even for $u = 0$. This is well understood in the context of monomer subdiffusion in polymers [60]. Again, for $u \neq 0$ this subdiffusive behavior remains without any change across the ST seen via many-body chaos. We expect the quantum model [Eq. (1)] to exhibit diffusion in the absence of measurements. It will be interesting to explore the subdiffusive behavior in the presence of measurements in the quantum limit and the connection between diffusion or subdiffusion with entanglement growth [61–63].

We now characterize the many-body chaos in the integrable classical Toda chain. The results for λ_L and v_B as a function of γ for the Toda chain with $a = 0.07$ and $b = 15.0$ are shown in Figs. 4(a) and 4(b) (see SM, Sec. S4 for more details [54]). As expected, the integrable limit with $\gamma = 0$ does not show any exponential growth, implying $\lambda_L = 0$. However, the cOTOC still exhibits ballistic spreading in this limit (Fig. S7 of SM), yielding a nonzero v_B as shown in Fig. 4(b).

As soon as γ becomes nonzero, the dynamics becomes chaotic with both exponential growth and ballistic spreading of cOTOC. As shown in Figs. 4(a) and 4(b), the extracted $\lambda_{\rm L}$ increases [64,65] rapidly as $\gamma^{0.3}$ and v_B exhibits a jump near the integrable limit with increasing γ. Thus, the integrable limit appears singular with respect to v_B for $\gamma \to 0^+$. Further increasing γ, v_B monotonically decreases and approaches zero at a critical $\gamma = \gamma_c$, indicating a transition to a nonchaotic phase. In contrast, $\lambda_{\rm L}$ shows a nonmonotonic dependence on γ, with a maximum at an intermediate γ. Nevertheless, $\lambda_{\rm L}$ eventually vanishes at γ_c, becoming negative for $\gamma > \gamma_c$, as in the nonintegrable model. Thus, the noise or dissipation, though initially making the integrable model chaotic, eventually destroys chaos due to the stochastic synchronization. The fact that $\lambda_{\rm L} = 0$ for $\gamma = 0$ and $\gamma > \gamma_c$, and $\lambda_{\rm L} > 0$ for small γ due to the breaking of intigribility [64,65], dictates that $\lambda_{\rm L}(\gamma)$ is nonmonotonic.

Discussions.—In summary, we show that effective dynamics of the position and momentum of the quantum oscillators under continuous weak position measurements maps to standard stochastic Langevin evolution in the semiclassical limit of small but nonzero $\hbar$. The Langevin dynamics for interacting chains, remarkably, exhibit ST in many-body chaos as a function of noise strength. The latter is controlled by the measurement strength in the parent quantum measurement model implying that the ST is an MIPT in the semiclassical limit.

The use of stochastic Langevin dynamics might suggest the absence of entanglement in the semicalssical limit. However, this naive inference is not correct. The semiclassical limit of entanglement needs to be taken carefully [66–68], where one first obtains an SK path integral for entanglement entropy, e.g., second Rényi entropy [69], in the quantum model and then takes the semiclassical limit. This results in effective dynamical equations for entanglement [70] different from Eq. (3). The latter only describes the effective dynamics of positions and momenta, as typically done in semiclassical approximations [71], and is useful for capturing OTOC (4) in the semiclassical limit. However, the connection between the growth of OTOC and entanglement has been shown in various situations [72–74]. Hence the ST transition in OTOC suggests an entanglement transition in the semiclassical limit.

The study of the MIPT in the fully quantum limit of our model will be an interesting future direction since systems of interacting oscillators under continuous measurements mimic many realistic open quantum systems. MIPTs have already been shown to exist for continuous weak measurements within more tractable quantum dynamics, like for quantum circuits [37,38], and noninteracting fermionic systems [7]. Moreover, there are several works [41–43] on the Bose-Hubbard model that show MIPT in the presence of measurements. The oscillator model in our Letter can be easily mapped to an interacting boson model.

Thus, quite generally, MIPT as a function of measurement strength is expected to occur in our models even in the fully quantum limit.

* sibaramr@iisc.ac.in
† sumilan@iisc.ac.in

[1] Brian Skinner, Jonathan Ruhman, and Adam Nahum, Measurement-induced phase transitions in the dynamics of entanglement, Phys. Rev. X **9**, 031009 (2019).

[2] Chao-Ming Jian, Yi-Zhuang You, Romain Vasseur, and Andreas W. W. Ludwig, Measurement-induced criticality in random quantum circuits, Phys. Rev. B **101**, 104302 (2020).

[3] Soonwon Choi, Yimu Bao, Xiao-Liang Qi, and Ehud Altman, Quantum error correction in scrambling dynamics and measurement-induced phase transition, Phys. Rev. Lett. **125**, 030505 (2020).

[4] Yaodong Li, Xiao Chen, and Matthew P. A. Fisher, Measurement-driven entanglement transition in hybrid quantum circuits, Phys. Rev. B **100**, 134306 (2019).

[5] Michael J. Gullans and David A. Huse, Dynamical purification phase transition induced by quantum measurements, Phys. Rev. X **10**, 041020 (2020).

[6] Adam Nahum, Sthitadhi Roy, Brian Skinner, and Jonathan Ruhman, Measurement and entanglement phase transitions in all-to-all quantum circuits, on quantum trees, and in Landau-Ginsburg theory, PRX Quantum **2**, 010352 (2021).

[7] O. Alberton, M. Buchhold, and S. Diehl, Entanglement transition in a monitored free-fermion chain: From extended criticality to area law, Phys. Rev. Lett. **126**, 170602 (2021).

[8] Shengqi Sang, Yaodong Li, Tianci Zhou, Xiao Chen, Timothy H. Hsieh, and Matthew P. A. Fisher, Entanglement negativity at measurement-induced criticality, PRX Quantum **2**, 030313 (2021).

[9] Shao-Kai Jian, Chunxiao Liu, Xiao Chen, Brian Swingle, and Pengfei Zhang, Measurement-induced phase transition in the monitored Sachdev-Ye-Kitaev model, Phys. Rev. Lett. **127**, 140601 (2021).

[10] Maxwell Block, Yimu Bao, Soonwon Choi, Ehud Altman, and Norman Y. Yao, Measurement-induced transition in long-range interacting quantum circuits, Phys. Rev. Lett. **128**, 010604 (2022).

[11] A. Zabalo, M. J. Gullans, J. H. Wilson, R. Vasseur, A. W. W. Ludwig, S. Gopalakrishnan, David A. Huse, and J. H. Pixley, Operator scaling dimensions and multifractality at measurement-induced transitions, Phys. Rev. Lett. **128**, 050602 (2022).

[12] Fergus Barratt, Utkarsh Agrawal, Sarang Gopalakrishnan, David A. Huse, Romain Vasseur, and Andrew C. Potter, Field theory of charge sharpening in symmetric monitored quantum circuits, Phys. Rev. Lett. **129**, 120604 (2022).

[13] K. Matsumoto and I. Tsuda, Noise-induced order, J. Stat. Phys. **31**, 87 (1983).

[14] S. Fahy and D. R. Hamann, Transition from chaotic to nonchaotic behavior in randomly driven systems, Phys. Rev. Lett. **69**, 761 (1992).

[15] Amos Maritan and Jayanth R. Banavar, Chaos, noise, and synchronization, Phys. Rev. Lett. **72**, 1451 (1994).

[16] Sunghwan Rim, Dong-Uk Hwang, Inbo Kim, and Chil-Min Kim, Chaotic transition of random dynamical systems and chaos synchronization by common noises, Phys. Rev. Lett. **85**, 2304 (2000).

[17] Changsong Zhou and Jürgen Kurths, Noise-induced phase synchronization and synchronization transitions in chaotic oscillators, Phys. Rev. Lett. **88**, 230602 (2002).

[18] Peter Grassberger, Synchronization of coupled systems with spatiotemporal chaos, Phys. Rev. E **59**, R2520 (1999).

[19] Franco Bagnoli, Lucia Baroni, and Paolo Palmerini, Synchronization and directed percolation in coupled map lattices, Phys. Rev. E **59**, 409 (1999).

[20] Lucia Baroni, Roberto Livi, and Alessandro Torcini, Transition to stochastic synchronization in spatially extended systems, Phys. Rev. E **63**, 036226 (2001).

[21] Massimo Cencini and Alessandro Torcini, Linear and nonlinear information flow in spatially extended systems, Phys. Rev. E **63**, 056201 (2001).

[22] Volker Ahlers and Arkady Pikovsky, Critical properties of the synchronization transition in space-time chaos, Phys. Rev. Lett. **88**, 254101 (2002).

[23] F. Ginelli, R. Livi, A. Politi, and A. Torcini, Relationship between directed percolation and the synchronization transition in spatially extended systems, Phys. Rev. E **67**, 046217 (2003).

[24] Miguel A. Muñoz and Romualdo Pastor-Satorras, Stochastic theory of synchronization transitions in extended systems, Phys. Rev. Lett. **90**, 204101 (2003).

[25] Franco Bagnoli and Raúl Rechtman, Synchronization universality classes and stability of smooth coupled map lattices, Phys. Rev. E **73**, 026202 (2006).

[26] A. Pikovsky, M. G. Rosenblum, and J. Kurths, *Synchronization, A Universal Concept in Nonlinear Sciences* (Cambridge University Press, Cambridge, England, 2001).

[27] Morikazu Toda, Wave propagation in anharmonic lattices, J. Phys. Soc. Jpn. **23**, 501 (1967).

[28] M. Hénon, Integrals of the Toda lattice, Phys. Rev. B **9**, 1921 (1974).

[29] Hermann Flaschka, The Toda lattice. II. Existence of integrals, Phys. Rev. B **9**, 1924 (1974).

[30] Hermann Flaschka, On the Toda lattice. II: Inverse-scattering solution, Prog. Theor. Phys. **51**, 703 (1974).

[31] M. Cencini, C. J. Tessone, and A. Torcini, Chaotic synchronizations of spatially extended systems as nonequilibrium phase transitions, Chaos **18**, 037125 (2008).

[32] Francesco Ginelli, Massimo Cencini, and Alessandro Torcini, Synchronization of spatio-temporal chaos as an absorbing phase transition: A study in $2 + 1$ dimensions, J. Stat. Mech. (2009) P12018.

[33] Josef Willsher, Shu-Wei Liu, Roderich Moessner, and Johannes Knolle, Measurement-induced phase transition in a chaotic classical many-body system, Phys. Rev. B **106**, 024305 (2022).

[34] Aydin Deger, Sthitadhi Roy, and Achilleas Lazarides, Arresting classical many-body chaos by kinetic constraints, Phys. Rev. Lett. **129**, 160601 (2022).

[35] Aydin Deger, Achilleas Lazarides, and Sthitadhi Roy, Constrained dynamics and directed percolation, Phys. Rev. Lett. **129**, 190601 (2022).

[36] Anasuya Lyons, Soonwon Choi, and Ehud Altman, A universal crossover in quantum circuits governed by a proximate classical error correction transition, Phys. Rev. B **107**, 174304 (2023).

[37] M. Szyniszewski, A. Romito, and H. Schomerus, Entanglement transition from variable-strength weak measurements, Phys. Rev. B **100**, 064204 (2019).

[38] M. Szyniszewski, A. Romito, and H. Schomerus, Universality of entanglement transitions from stroboscopic to continuous measurements, Phys. Rev. Lett. **125**, 210602 (2020).

[39] Xiangyu Cao, Antoine Tilloy, and Andrea De Luca, Entanglement in a fermion chain under continuous monitoring, SciPost Phys. **7**, 024 (2019).

[40] Xiao Chen, Yaodong Li, Matthew P. A. Fisher, and Andrew Lucas, Emergent conformal symmetry in nonunitary random dynamics of free fermions, Phys. Rev. Res. **2**, 033017 (2020).

[41] Qicheng Tang and W. Zhu, Measurement-induced phase transition: A case study in the nonintegrable model by density-matrix renormalization group calculations, Phys. Rev. Res. **2**, 013022 (2020).

[42] Yohei Fuji and Yuto Ashida, Measurement-induced quantum criticality under continuous monitoring, Phys. Rev. B **102**, 054302 (2020).

[43] Shimpei Goto and Ippei Danshita, Measurement-induced transitions of the entanglement scaling law in ultracold gases with controllable dissipation, Phys. Rev. A **102**, 033316 (2020).

[44] Samuel J. Garratt, Zack Weinstein, and Ehud Altman, Measurements conspire nonlocally to restructure critical quantum states, Phys. Rev. X **13**, 021026 (2023).

[45] Avijit Das, Saurish Chakrabarty, Abhishek Dhar, Anupam Kundu, David A. Huse, Roderich Moessner, Samriddhi Sankar Ray, and Subhro Bhattacharjee, Light-cone spreading of perturbations and the butterfly effect in a classical spin chain, Phys. Rev. Lett. **121**, 024101 (2018).

[46] Thomas Bilitewski, Subhro Bhattacharjee, and Roderich Moessner, Temperature dependence of the butterfly effect in a classical many-body system, Phys. Rev. Lett. **121**, 250602 (2018).

[47] Amit Kumar Chatterjee, Anupam Kundu, and Manas Kulkarni, Spatiotemporal spread of perturbations in a driven dissipative duffing chain: An out-of-time-ordered correlator approach, Phys. Rev. E **102**, 052103 (2020).

[48] Sibaram Ruidas and Sumilan Banerjee, Many-body chaos and anomalous diffusion across thermal phase transitions in two dimensions, SciPost Phys. **11**, 087 (2021).

[49] Sugan Durai Murugan, Dheeraj Kumar, Subhro Bhattacharjee, and Samriddhi Sankar Ray, Many-body chaos in thermalized fluids, Phys. Rev. Lett. **127**, 124501 (2021).

[50] Thomas Bilitewski, Subhro Bhattacharjee, and Roderich Moessner, Classical many-body chaos with and without quasiparticles, Phys. Rev. B **103**, 174302 (2021).

[51] Shu-Wei Liu, J. Willsher, T. Bilitewski, Jin-Jie Li, A. Smith, K. Christensen, R. Moessner, and J. Knolle, Butterfly effect and spatial structure of information spreading in a chaotic cellular automaton, Phys. Rev. B **103**, 094109 (2021).

[52] Carlton M. Caves and G. J. Milburn, Quantum-mechanical model for continuous position measurements, Phys. Rev. A **36**, 5543 (1987).

[53] Aritra Kundu and Abhishek Dhar, Equilibrium dynamical correlations in the Toda chain and other integrable models, Phys. Rev. E **94**, 062130 (2016).

[54] See Supplemental Material at http://link.aps.org/supplemental/10.1103/PhysRevLett.132.030402 for additional details of the derivation of the Schwinger-Keldysh path integral for quantum measurement model and its semiclassical limit, details of the numerical simulation of stochastic Langevin equation and finite size scaling, and supplemental plots of OTOC, light cone and mean square displacement.

[55] Nicolas Gisin and Ian C Percival, Quantum state diffusion, localization and quantum dispersion entropy, J. Phys. A **26**, 2233 (1993).

[56] L. Diósi, N. Gisin, and W. T. Strunz, Non-Markovian quantum state diffusion, Phys. Rev. A **58**, 1699 (1998).

[57] Alex Kamenev, *Field Theory of Non-Equilibrium Systems* (Cambridge University Press, Cambridge, England, 2011).

[58] W. F. Van Gunsteren and H. J. C. Berendsen, Algorithms for Brownian dynamics, Mol. Phys. **45**, 637 (1982).

[59] J. Florencio and M. Howard Lee, Exact time evolution of a classical harmonic-oscillator chain, Phys. Rev. A **31**, 3231 (1985).

[60] Stephanie C. Weber, Julie A. Theriot, and Andrew J. Spakowitz, Subdiffusive motion of a polymer composed of subdiffusive monomers, Phys. Rev. E **82**, 011913 (2010).

[61] Tibor Rakovszky, Frank Pollmann, and C. W. von Keyserlingk, Sub-ballistic growth of Rényi entropies due to diffusion, Phys. Rev. Lett. **122**, 250602 (2019).

[62] Tianci Zhou and Andreas W. W. Ludwig, Diffusive scaling of Rényi entanglement entropy, Phys. Rev. Res. **2**, 033020 (2020).

[63] Marko Žnidarič, Entanglement growth in diffusive systems, Commun. Phys. **3**, 100 (2020).

[64] Khanh-Dang Nguyen Thu Lam and Jorge Kurchan, Stochastic perturbation of integrable systems: A window to weakly chaotic systems, arXiv:1305.4503.

[65] Tomer Goldfriend and Jorge Kurchan, Quasi-integrable systems are slow to thermalize but may be good scramblers, Phys. Rev. E **102**, 022201 (2020).

[66] Renato M. Angelo and K. Furuya, Semiclassical limit of the entanglement in closed pure systems, Phys. Rev. A **71**, 042321 (2005).

[67] A. Matzkin, Entanglement in the classical limit: Quantum correlations from classical probabilities, Phys. Rev. A **84**, 022111 (2011).

[68] G. Mussardo and J. Viti, $\hbar \to 0$ limit of the entanglement entropy, Phys. Rev. A **105**, 032404 (2022).

[69] Arijit Haldar, Surajit Bera, and Sumilan Banerjee, Rényi entanglement entropy of Fermi and non-Fermi liquids: Sachdev-Ye-Kitaev model and dynamical mean field theories, Phys. Rev. Res. **2**, 033505 (2020).

[70] S. Banerjee (unpublished).

[71] Anatoli Polkovnikov, Phase space representation of quantum dynamics, Ann. Phys. (Amsterdam) **325**, 1790 (2010).

[72] Pavan Hosur, Xiao-Liang Qi, Daniel A. Roberts, and Beni Yoshida, Chaos in quantum channels, J. High Energy Phys. 02 (2016) 004.

[73] Ruihua Fan, Pengfei Zhang, Huitao Shen, and Hui Zhai, Out-of-time-order correlation for many-body localization, Sci. Bull. **62**, 707 (2017).

[74] Akram Touil and Sebastian Deffner, Quantum scrambling and the growth of mutual information, Quantum Sci. Technol. **5**, 035005 (2020).